STScI | SPACE TELESCOPE SCIENCE INSTITUTE

JWST TECHNICAL REPORT

Title: NIRISS Commissioning Results: NIS-009 Detector Gain and Linearity (NGAS CAR-348, APT 1084)	Doc #: JWST-STScI-008277, SM-12 Date: 7 October 2022 Rev: -
Authors: Rachel Cooper, Kevin Volk, the NIRISS team Phone: 410-338-6847	Release Date: 31 March 2023

1 Abstract

The gain value of the NIRISS detector was measured with the standard photon transfer method for each of the four detector channels and compared to the appropriate ground-based measurements. The in-flight gain measurement was found to be within 5% of the CV3 internal and external lamp flat-derived gain values, so no updates to reference files are needed at this time. The coefficients for the linearity correction were also verified by checking that linearized ramps do not exhibit curvature that would indicate a problem with the current linearity coefficients.

2 Introduction

Internal flat fields were collected to measure the gain of each of the four channels of the NIRISS detector as well as the linearity correction coefficients of each pixel. Because of the small instabilities in the lamp flux, the measurements were not expected be of sufficient quality to calibrate the science data. Any large deviation in the values of the gain and linearity coefficients from those measured in the ground campaigns would indicate a problem with the detector electronics.

All NIRISS exposures utilize an intermediate conversion from counts to electrons via the gain as part of the data reduction process. The gain value was measured with the standard photon transfer method for each of the four detector channels and compared to values from ground-based testing campaigns. If found to be significantly different, the gain reference file would need to be updated and the new values propagated into the JWST calibration pipeline for processing the science observations. The coefficients for the linearity correction were also calculated with standard software packages developed by the NIRISS team.

3 Exposures

Table 1: Full-frame internal flats taken for NIS-009 gain and linearity analysis

Obs #	Filter	Lamp Name	Lamp Power	Groups/Int	Ints/Exp	Total Exposure Time
1	F200W	LINE2	OFF	50	3	1642.726
2	F200W	LINE2	LEVEL5	50	3	1642.726
3	F200W	LINE2	LEVEL5	50	3	1642.726
4	F200W	LINE2	LEVEL5	10	5	590.522
5	F200W	LINE2	LEVEL6	30	3	998.52
6	F200W	LINE2	OFF	10	3	354.313

Determining the integration time (or number of groups) necessary to reach the full well with the LINE2 lamp at a specified lamp LEVEL in F200W + CLEAR is no easy task because of the highly non-uniform pedestal or "bias" level of the detector and illumination of the lamp on the detector. From a full-frame dark, the bias level is about 9000-22000 ADUs with a median of about 12000 ADUs. The range of the count rate of the LINE2 lamp at LEVEL5 is about 410-1030 ADUs/group (corner to corner), offering decent sampling for linearity calculations. Including the bias level, counts of 30000-64200 ADUs can be reached in 50 groups. This range corresponds to about 48000-102000 e- for a gain of 1.6 e-/ADU, thus reaching the full well of 100000 e- in some portions of the detector while remaining below the digital saturation.

To reach a larger dynamic range in the other pixels (while saturating part of the field), however, the number of groups or the lamp level needs to be increased. We choose to increase the lamp level since more groups would make the exposures prohibitively long. A LINE2/LEVEL6 exposure shows a coarser count rate of about 2.7 times that of LINE2/LEVEL5, i.e., 1100-2700 ADUs/group, and so 30 groups at LEVEL6 would produce counts of 42000-92200 ADUs in the last group. The regions with the lowest count rates, primarily along the perimeter of the detector, will be below saturation while the central regions of the field will fill the full well and reach digital saturation.

We sequence three background integrations, six internal flat integrations at LINE2/LEVEL5, five at LINE2/LEVEL5 but with a smaller number of groups to increase the S/N ratio at lower counts, three with LINE2/LEVEL6, and another three background integrations (but shorter) to characterize any persistence. Since the lamp is turned off at the end of each exposure, not between integrations, we prefer NEXP = 1 with several NINTS to allow the lamp to stabilize (and minimize the overhead in time) while staying below the maximum lamp-on time of 2000 sec. As discussed in NIS-007 Calibration Lamps Verification (1082), we prefer to remain at LEVEL5 (or higher) to avoid instabilities and settling time in the lamp flux. The multiple integrations will also help remove CR hits not identified by the JWST calibration pipeline.

The configuration of the exposures taken during this program are summarized in Table 1. From APT, the science time is 1.8 hours and the charged time is 2.9 hours. The total data volume of the exposures in this activity is about 5.2 GB.

4 Analysis Plan

We performed the following steps to verify the exposures described above:

1. Confirm all expected data products available on MAST.
2. Check uncalibrated file FITS headers correct (nis_comm.utils.check_niriss_headers.py)
3. Play through all groups/integrations in DS9 to check for obvious problems

4.1 Gain

As noted in JWST-STScI-004823, the NIRISS internal lamps are less stable than the CV3 OSIM source and therefore provide less even detector illumination, so while the gain will be measured in flight, it is expected that the CV3 gain map will remain in use during JWST operations. The details of the algorithm used to determine the detector gain, the photon transfer method, are provided in more detail in JWST-STScI-004823 (Analysis of NIRISS CV3 Data: Detector Gain Measurements) and references therein. The code to calculate gain and produce the pipeline-compliant reference file is stored on the NIRISS GitLab gain reference file creation repository. Further details on the calculation of the gain and creation of the gain reference file are given in JWST-STScI-005661 (Description of the Gain Reference File). The data analysis procedure executed with the data from NIS-009, PID 1084, is as follows:

1. Truncate ramps below 10k counts per group if necessary, using the reffile_tools.truncate_ramp() function to write out to ramps to new fits files
2. Run gain_ref_file.py to calculate gain using the photon transfer method and produce the gain reference file. The following steps are performed by the code.
    a. Run the JWST Detector1Pipeline, performing only the superbias subtraction and reference pixel correction steps on each input exposure, and write out each ramp (integration) to a separate file. Update run_pipeline.py to use new superbias reference file produced in NAP-006.
    b. Compute the mean gain in 20 x 20 pixel tiles covering the inner 2040x2040 pixels of the detector image (102 x 102 tiles)
    c. Restore the gain map to its full size, add reference pixels, and apply a series of corrections to the gain value: IPC correction, bad spot patching, and Gaussian smoothing
    d. Produce the final gain reference file and verify for CRDS format compliance (technical verification)
3. Compare to gain reference file **and** to gain map(s) produced from internal flats:
    a. CV3 OSIM flat gain map reference file (GitLab code)
    b. CV3 internal flat gain maps (Martel's code):
        i. Level 5 lamp, 10 groups, 3 integrations
        ii. Level 6 lamp, 35 groups, 3 integrations
    c. CV3 internal flat gain maps (GitLab code):
        i. Level 5 lamp, 10 groups, 3 integrations, with and without smoothing
        ii. Level 6 lamp, 35 groups, 3 integrations, with and without smoothing

d. CV3 OSIM flat gain map using only 3 integrations (of 224)
e. Produce histogram of gain in illuminated detector area, and histograms of the gain in the four detector channels. Compare mean gain values to reference file.
f. Produce residual image of current reference file minus commissioning gain map; check for structure and other anomalies

4.2 Linearity

As with the gain portion of NIS-009, the linearity measurement is not expected to be as precise as the ground cryo-vac campaign measurements due to lamp instability. However, linearity test ramps can be run through the pipeline and the pixel-by-pixel ramp curvature examined. This will be zero for perfectly linearized ramps, so any significant deviations from zero curvature will be a possible sign of issues in the linearity coefficients. In practice the curvature of a set of points is measured by the inverse radius of curvature (kappa) so one wants a small kappa value from the ramps. It is not clear pre-flight if we can differentiate curvature from any possible variations in the lamp output over the ramp from curvature from the linearity correction.

5 Analysis Results

The steps above were followed to measure the in-flight detector gain and linearity. Level 1a (uncal) and 2a (rate, rateints) FITS files were present and downloaded from MAST. Basic header keyword checks performed on uncalibrated files passed with no missing or incorrect keys/values, with the exception of the DURATION and EFFEXPTM values, which differ slightly from the expected times due to discrepant rounding (known issue documented on JIRA JWSTOSS-7663).

5.1 Gain

Of the 6 exposures taken in Program 1084, two lamp-on internal flats with LINE2 lamp at LEVEL5 were used to calculate the detector gain. Their basic details are given in Table 2.

Table 2: Two exposures used for gain analysis

Filename	DATE-OBS	TIME-OBS	EFFEXPTM
jw01084001001_02102_00001_nis	2022-04-21	12:22:06.035	1610.52 s
jw01084001001_02103_00001_nis	2022-04-21	12:52:38.673	1610.52 s

No obvious visual anomalies or lamp failures were found in a preliminary examination of these to exposures using DS9. Ramps were trimmed after 12 groups to stay below a mean signal level of 10,000 ADU per pixel. The JWST Detector1 pipeline reference pixel, linearity, and superbias steps were run, overriding the superbias reference file selection in order to use the in-flight superbias which was not yet active in CRDS at that time.

Then the procedure for calculating the gain as outlined in section 4.1 above was

followed to produce a new gain reference file. Only the IPC correction and patching were applied as post-processing correction to the final product; the smoothing step was skipped. The median gain across the NIRISS detector was calculated to be 1.536 ± 0.064 e-/ADU, where the quoted uncertainty is the standard deviation. The distribution of gain values is fairly well-represented by a normal distribution, as shown in Figure 1. The original analysis of the CV3 external flat data as reported in Volk 2017 (JWST-STScI-004823) found that the sum of two Gaussian distributions better represented the data. However, since that measurement is of much higher precision (a total of 224 ramps used, versus 6 used for the NIS-009 measurement), it is possible that the underlying distribution of these data is similarly bimodal but that it is lost in the noise. There does appear to be leftward peak to the histogram, but if there are two distinct populations present, they are very close in mean.

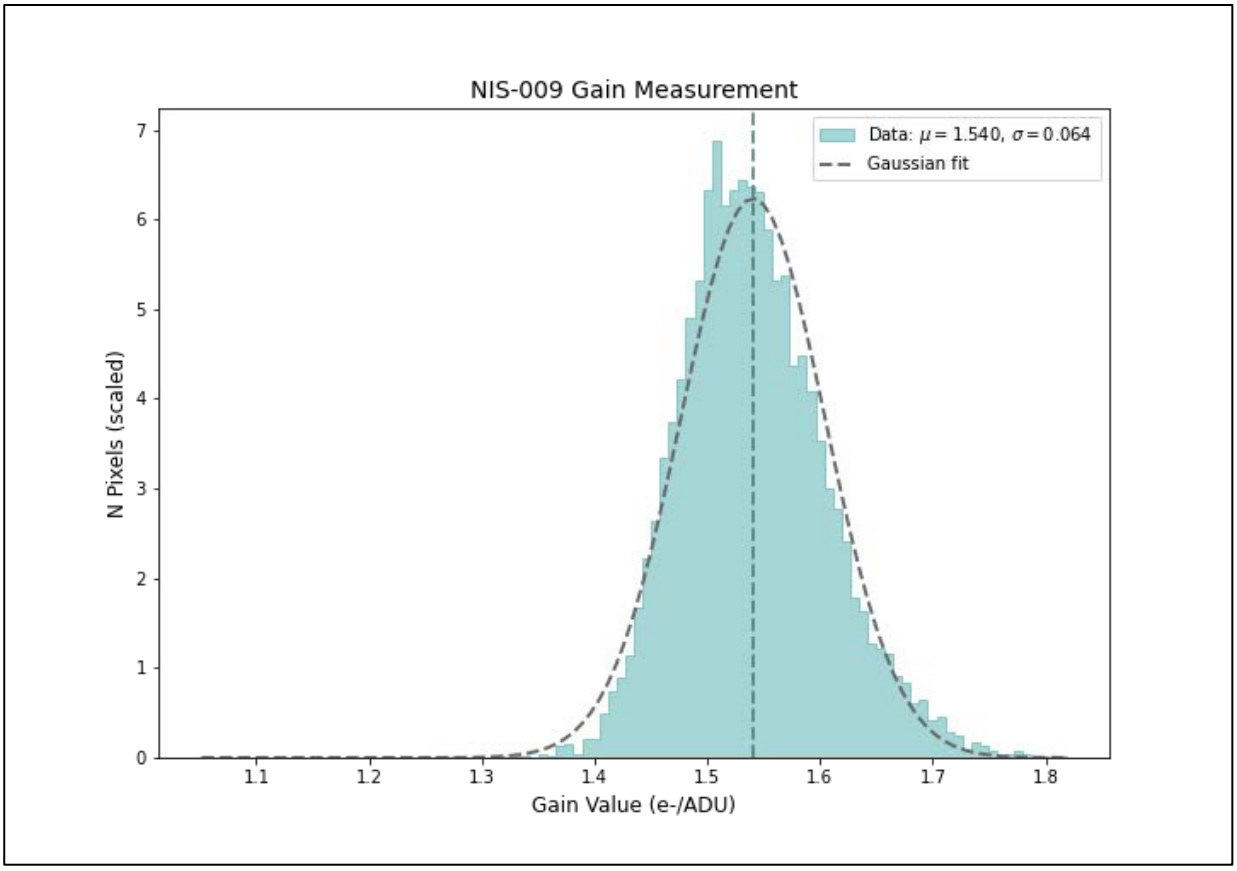

Figure 1: Histogram of gain values in the illuminated portion of the NIRISS detector measured from NIS-009, plotted with a single-component Gaussian fit to the data.

The histograms for the individual amplifier channels are plotted in Figure 2, with the channels ordered in the figure to correspond to their physical locations in the detector. While the mean gain varies slightly from channel to channel, with Channel D having the largest mean and standard deviation, the channel means are all within one sigma of each other. Gaussian fits to each channel are shown with dashed lines. Some basic statistics of each channel are also given in Table 2.

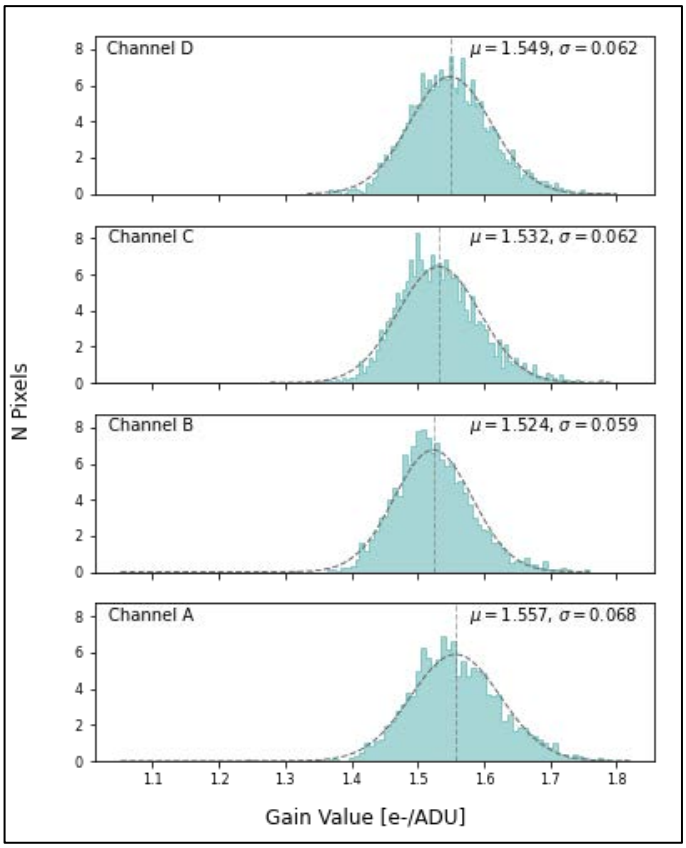

Figure 2: Histograms of the gain values in the four detector amplifier channels.

Table 3: Summary statistics for each channel of the in-flight gain map

Channel	Mean	Median	Std. Dev	Min	Max
A	1.54925	1.54653	0.0615499	1.33279	1.79807
B	1.53195	1.5265	0.0620694	1.27732	1.79005
C	1.52361	1.5188	0.0590307	1.05158	1.75881
D	1.55709	1.55113	0.0675275	1.05158	1.8181

A gradient in the gain value is noticeable across the detector, with the mean gain from the rightmost vertical quarter of the detector ~5 % higher than the leftmost quarter. The shape of the epoxy void is also visible in the gain map due to the imperfect correction for slightly lower intra-pixel capacitance in the void vs. non-void regions (see Figure 3). The structure is consistent with what was seen in ground measurements of the gain.

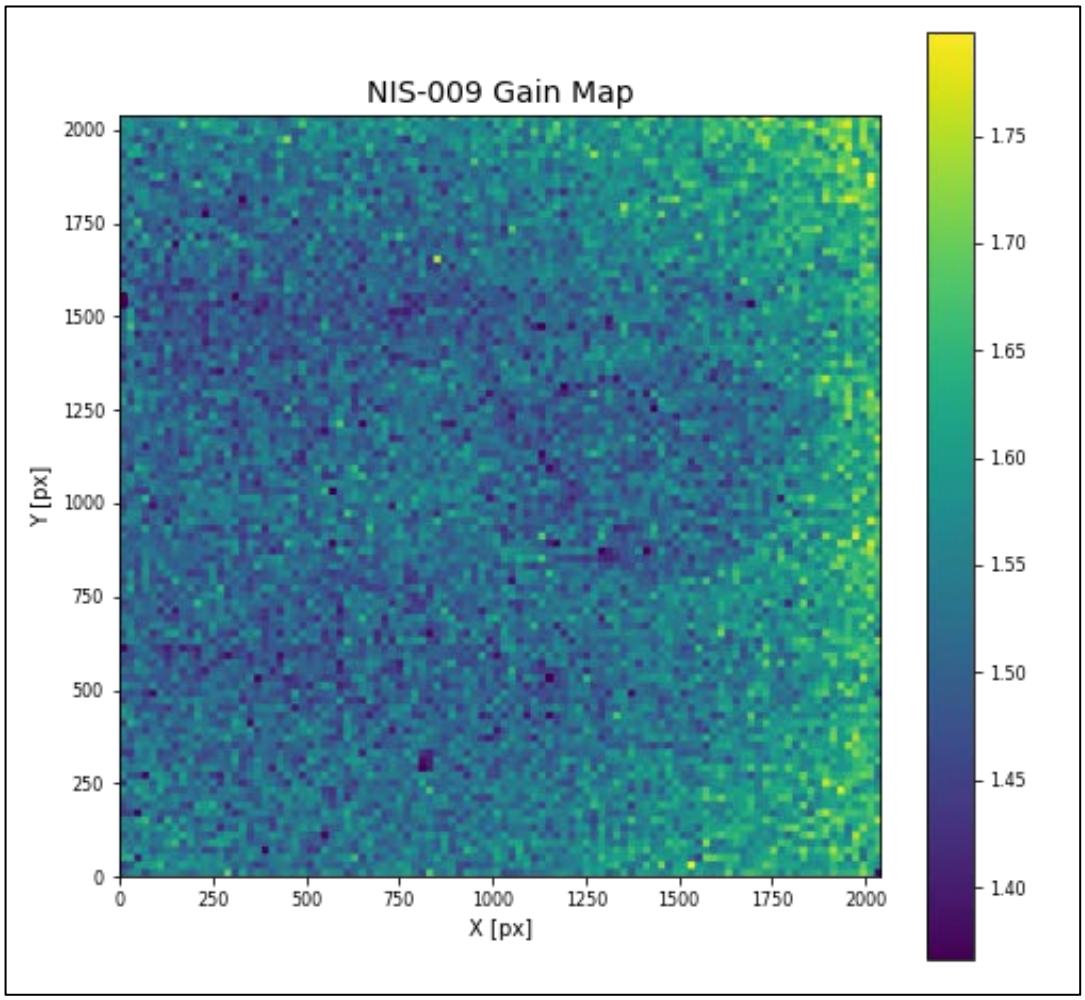

Figure 3: Gain map from NIRISS internal flat fields taken for NIS-009. The shape of the void is visible, as well as a gradient in the gain increasing from left to right. Both features are consistent with ground-based measurements.

The mean gain observed from the CV3 campaign linearity monitoring external flats was 1.622 ± 0.04 electrons/DN. This is the value currently used by the JWST calibration pipeline and assumed by a variety of secondary applications. We compare this value, as well as the mean gain in each of the four detector amplifier channels, to the equivalent values derived from CV3 internal-lamp flats and the in-flight NIS-009 flats.

The lengths and number of ramps used to measure the gain for the four gain maps being compared to the NIS-009 measurement are shown in Table 4. Example ramps from each data set are plotted in Figure 4, with the exception of the CV3 external 3-integration data (CV3 external 2), since the ramps used were just a subset of those used for the full calculation (CV3 external 1). The mean signal per group in an individual integration is shown to demonstrate the differences between the data sets used for comparison. The ramps shown have already been truncated below 10,000 ADU/pixel mean signal to exclude potentially nonlinear sections, where applicable.

Table 4: Summary of the input ramps to each gain value used as a comparison to the NIS-009 measurement.

Data Set	Groups	Integrations	Exposures	Total Ramps
NIS-009	12/50	3	2	6
CV3 External 1	6	28	8	224
CV3 External 2	6	3	1	3
CV3 Internal 1	10	3	1	3
CV3 Internal 2	6/35	3	1	3

Prior to the execution of this commissioning program, work was done to confirm that the gain calculation code hosted on GitLab produced results consistent with legacy code used to calculate previous versions of the gain map when using the same CV3 external lamp data. The results of this work are summarized in the Technical Report JWST-STScI-005661. This procedure was repeated ahead of NIS-009 with CV3 *internal* lamp data. Gain maps using CV3 internal 10- and 35-group data processed by André Martel were compared to gain maps using the same data processed with the GitLab code and the mean gain found to be consistent within 1σ. Therefore, for an apples-to-apples comparison of gain measurements from different data sets, the same GitLab code was used to calculate the gain for all the comparison gain maps discussed in this report. One difference between the gain maps discussed is the post-processing corrections applied; the CV3 external flat gain map delivered to CRDS has Gaussian smoothing applied to soften borders between the 20x20-pixel tiles on which the gain is calculated. This smoothing step was not applied to the other gain maps because it does not significantly change the mean gain (and so it is still an appropriate point of comparison). The pixel-by-pixel map is not currently used by the JWST pipeline, only the mean gain is used, though this may change in the future.

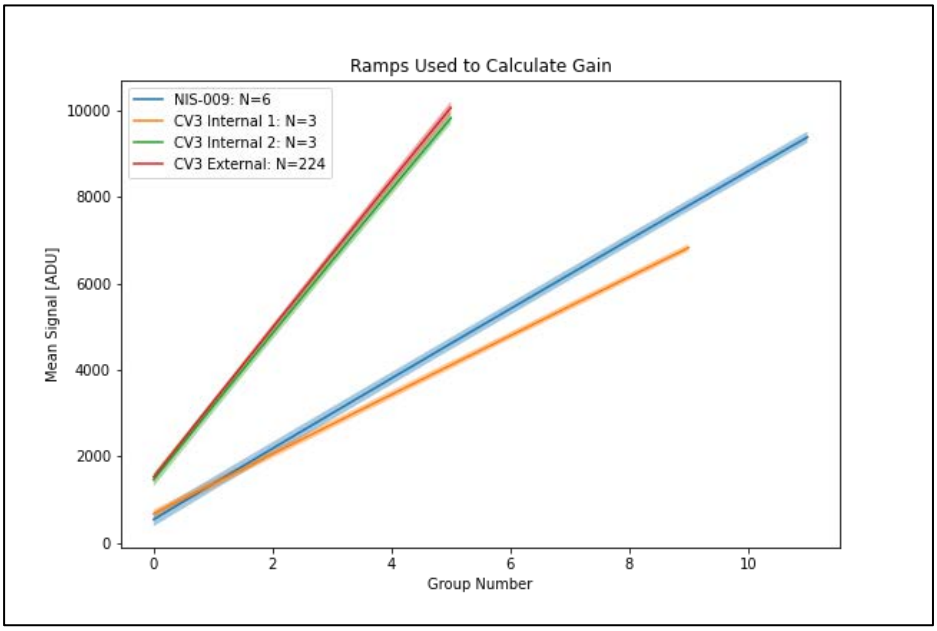

Figure 4: Comparison of the input ramps used to calculate the gain for NIS-009 and for three ground-testing data sets. All ramps have been truncated below a mean of 10,000 ADU per group. The mean ramp of each data set (N= number of ramps) is plotted with the standard deviation shown by the shaded region.

The distribution of gain values from the NIS-009 calculation compared to that of the four gain maps using CV3 data is explored in Figure 5. While NIS-009 median gain is the lowest of those plotted, the other medians fall within 1-sigma of the latest measurement. The latest measurement is ~2-3% lower than the measurements from the CV3 internal flat and a ~5% decrease from the current gain reference file. The gradient in gain value of approximately 5% between the leftmost and rightmost quarters of the detector is consistent with the same measurement from the CV3 gain maps.

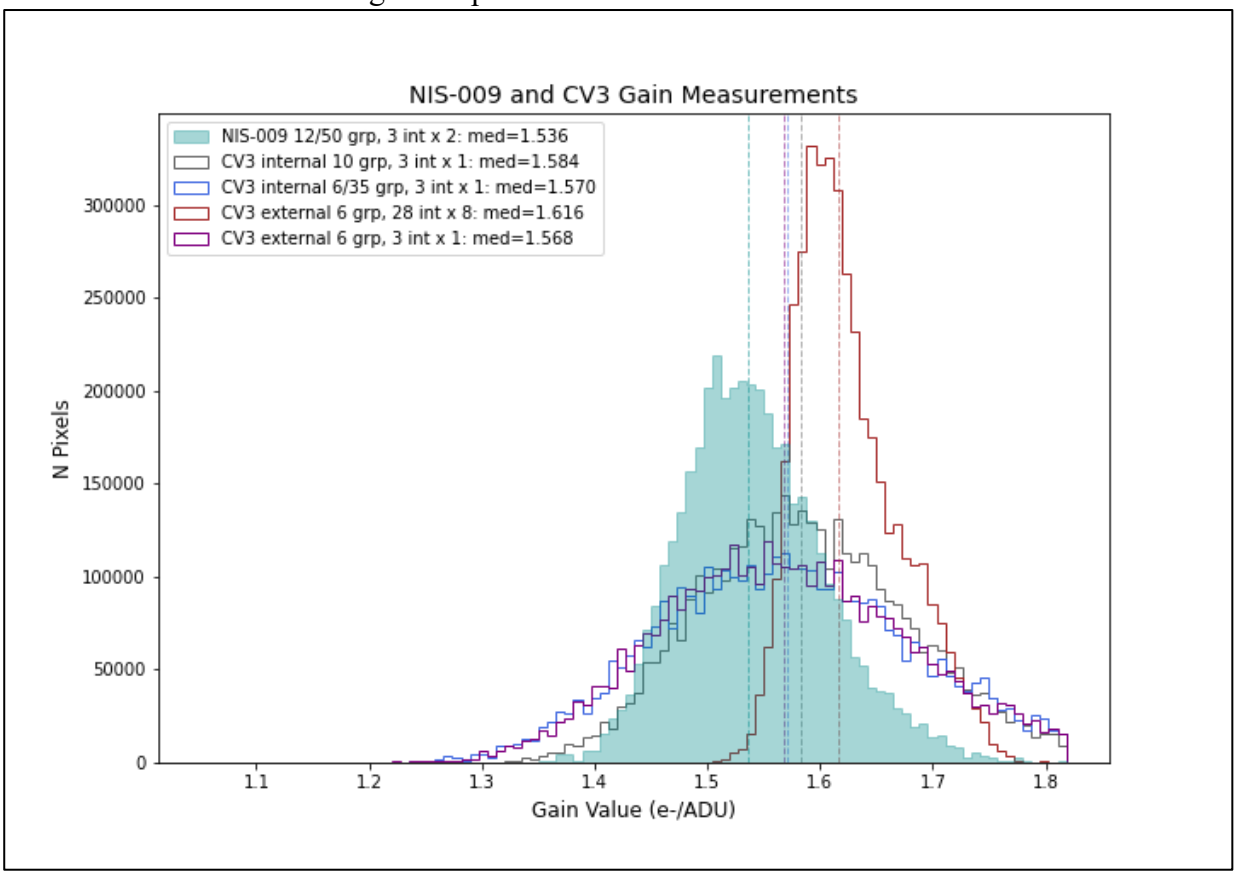

Figure 5: Comparison of gain histograms from NIS-009 and four gain measurements from CV3 data.

Residual images showed no unexpected structure; changes in the shape of the void since CV3 which were noticed in other commissioning analyses are not large enough to be visible in the residuals of the gain maps. The residual images of the NIS-009 map minus each of the comparison maps are shown in Figure 6. Two faint horizontal bands are visible in the residual images, approximately dividing the detector in thirds. These bands are not visible in the CV3 external flat gain map (224 ramps) but are visible in the ramp made using only 3 of those CV3 external flats, suggesting that it is a noise artifact. Distributions of the residual images were also examined and found to be roughly Gaussian.

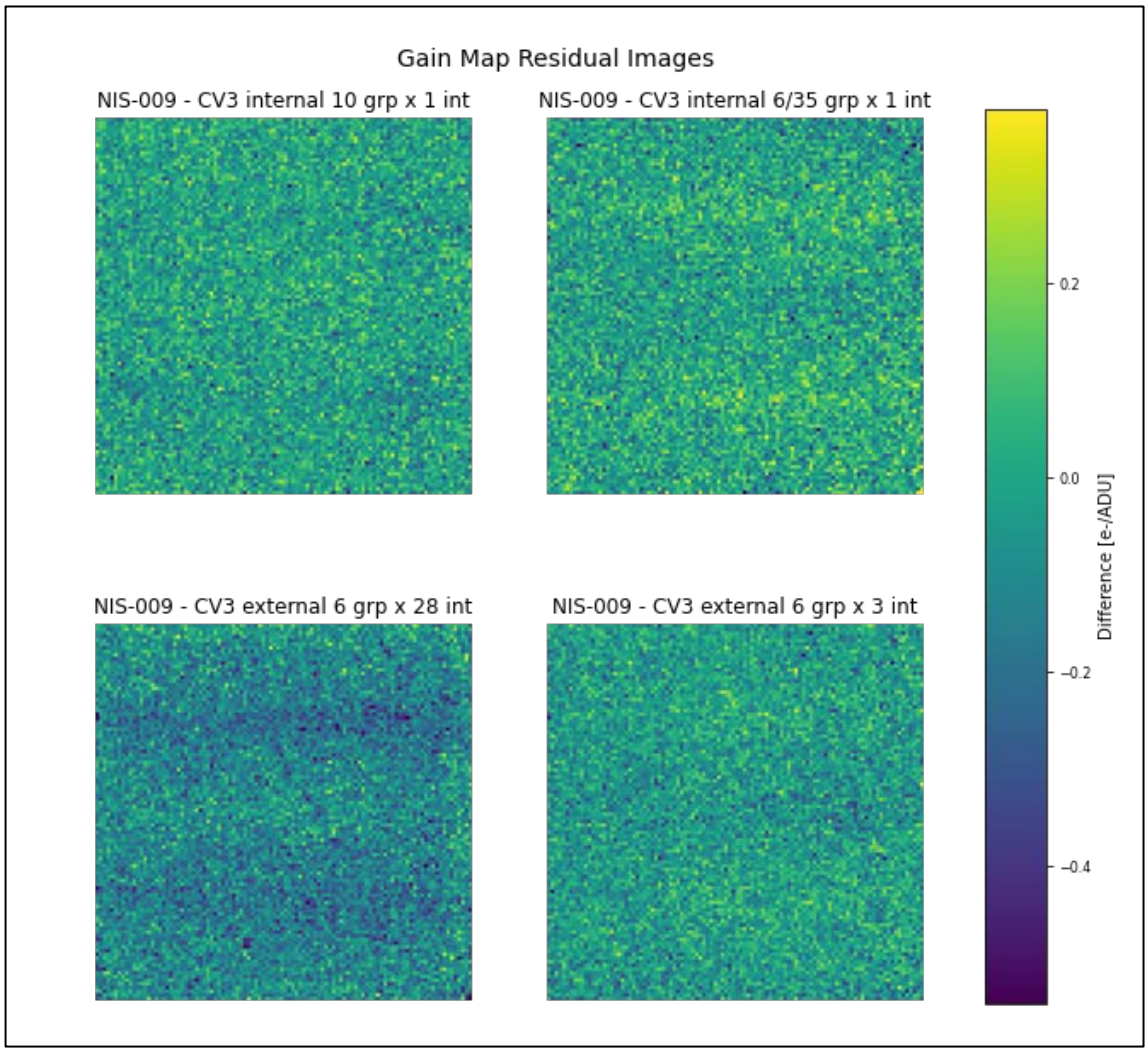

Figure 6: Residual gain maps of NIS-009 minus each of the CV3 gain maps used for comparison.

5.2 Linearity

The analysis of the ramp linearity was carried out on each of the lamp exposures using the code `ramp_curvature.py`. The code was applied to the data values in two forms: first, it was run on the stage 1 ("Detector1") pipeline output ramp from the linearity step; second, the code was also run on the first difference ramps generated from the linearized ramp. The first differences should define a flat line within the bounds of the uncertainties if the linearization is done correctly, and the output ramps from the linearity step should be linear as well. The test with the first differences is more sensitive than the test on the linearized ramps. In either case the output curvature values, κ, should be small. For the first difference ramps the κ values should be small compared to 1, and in the raw ramps the κ values should be small in absolute value. The κ values are calculated for each pair of points up the ramp, so for a ramp of N groups. One gets N−1 curvature estimates for a sample of N values. With multiple estimates there are various ways to estimate the ramp curvature. In the analysis here for each input ramp the code calculates the root-mean square relative deviations of the linearized ramps from the ideal linear ramps with the slopes defined in the output rate file from the pipeline, as well as all the individual κ values that were determined, the median κ values determined, and the maximum κ values per pixel per ramp. The measurements are made only on points up the ramps to the linearity correction limit so the number of samples per pixel varies somewhat over the image.

For each ramp of each lamp exposure the images of the median and maximum κ values were looked at to see whether any trends of concern were seen, and the histograms of values were also examined. As an illustration, the images and histograms for the first ramp in observation 3 are shown in Figure 7 to Figure 16.

The first image in Figure 7 shows the relative RMS ramp deviations in the first difference ramps, compared to the median signal per frame. The values are displayed using an IRAF zscale-type algorithm to set the range. This is needed because the bad pixels have large RMS deviations. The histogram is shown in the next figure. The peak RMS deviation is around 3%. The mean signal value over the image is about 76.3 ADU/s or roughly 1320 electrons/frame so the S/N per frame is about 36 purely from Poisson statistics, which matches the RMS deviation peak reasonably well. One does also see that the RMS deviations are larger in the lower corners where the illumination is lower (see Figure 15 below). This places a modest limit on the linearity deviations that can be present in the ramp. One does not see much structure in the RMS image aside from the variation caused by the illumination.

Looking next at the median curvature values in Figure 9 these tend to be around zero, indicating no overall failure of the linearity corrections. The mean value is $-2.3\ 10^{-10}$ with a standard deviation value of $1.27\ 10^{-8}$. The histogram is shown in Figure 10. The histogram is fairly symmetric about zero. Such small κ values indicate that there is no curvature in the ramps on the average.

Looking at the maximum κ values image and histogram one sees values of order a few times 10^{-7}, still rather small. There are some trends in the image. Again one sees an increase in

the maximum κ values as the illumination level decreases. There is the area of large κ values in a band in the upper left part of the image. This is odd but examination of ramps in this area did not show any systematic curvature that was visible to the eye.

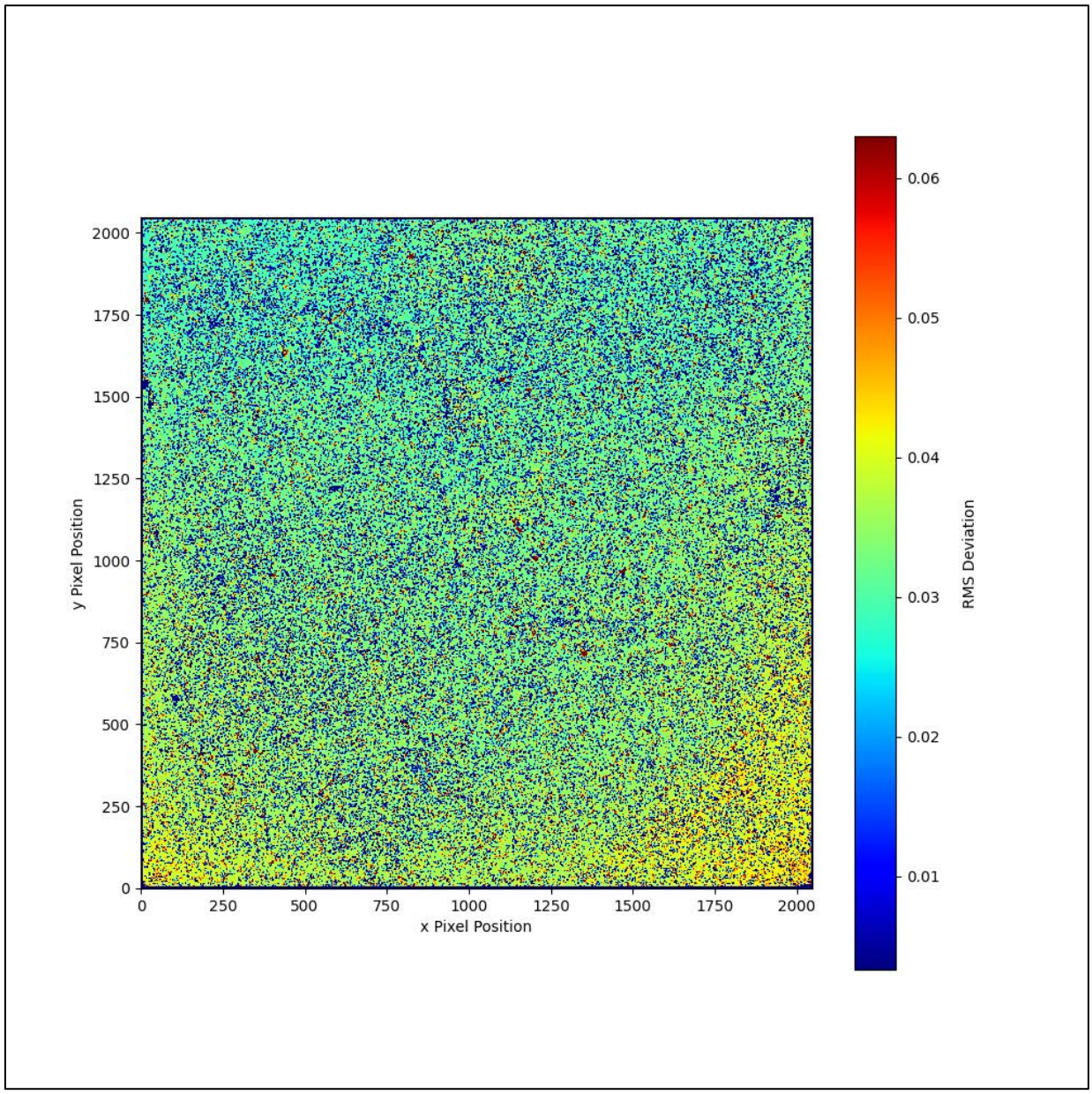

Figure 7: An example of the RMS deviation images derived from the ramps; this is for observation 3, ramp 1. These are the RMS relative deviations from a linear ramp with the slope in the rate image, calculated pixel by pixel.

Finally, the median curvature image for the first difference ramps is shown along with the histogram and then the first difference values for a randomly selected pixel. The maximum curvature values for the first difference ramps are always large because of the frame-to-frame fluctuations in the values, and so are not useful. The median curvature values are useful because if there is a systematic decrease of the first difference values up the ramp it will tend to

make the median curvature systematically negative. The median κ values fluctuate from pixel to pixel without any sign of large-scale structure in the image, and the histogram is both reasonably symmetric about zero and of fairly low magnitude. Hence this test also does not indicate any issues with the linearity coefficients in these observations.

A better test of the linearity would be obtained from repeated observations of a celestial source, since these sources are generally stable to a much higher degree than is the case for the NIRISS internal lamps. One would need to repeat such a observation many times to build up the S/N ratio and make a more accurate test of the linearity corrections. Such observations are beyond the scope of the commissioning activities.

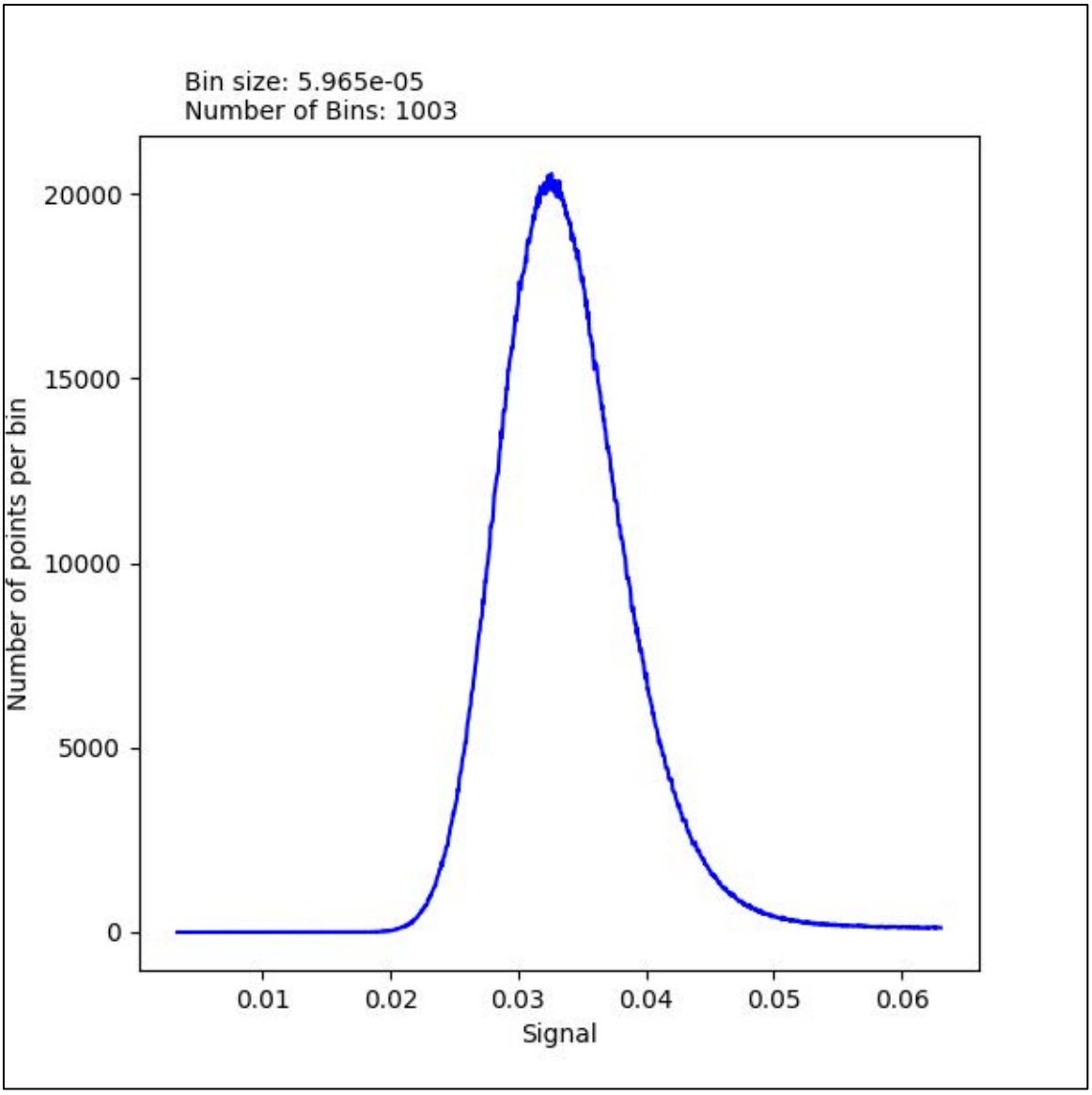

Figure 8: The histogram of the RMS values from Figure 7.

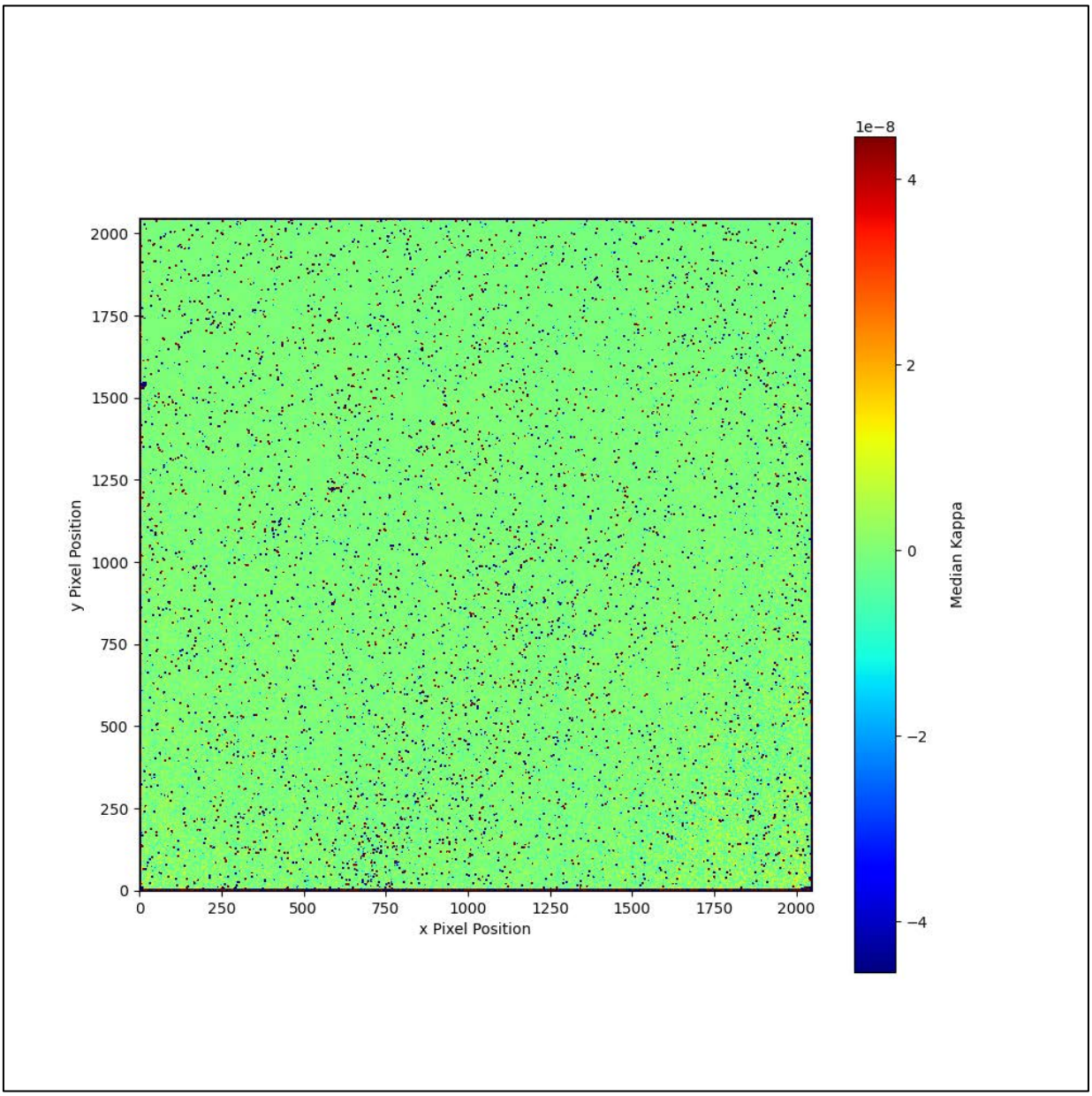

Figure 9: The pixel-by-pixel median curvature values found from ramp 1 of observation 3.

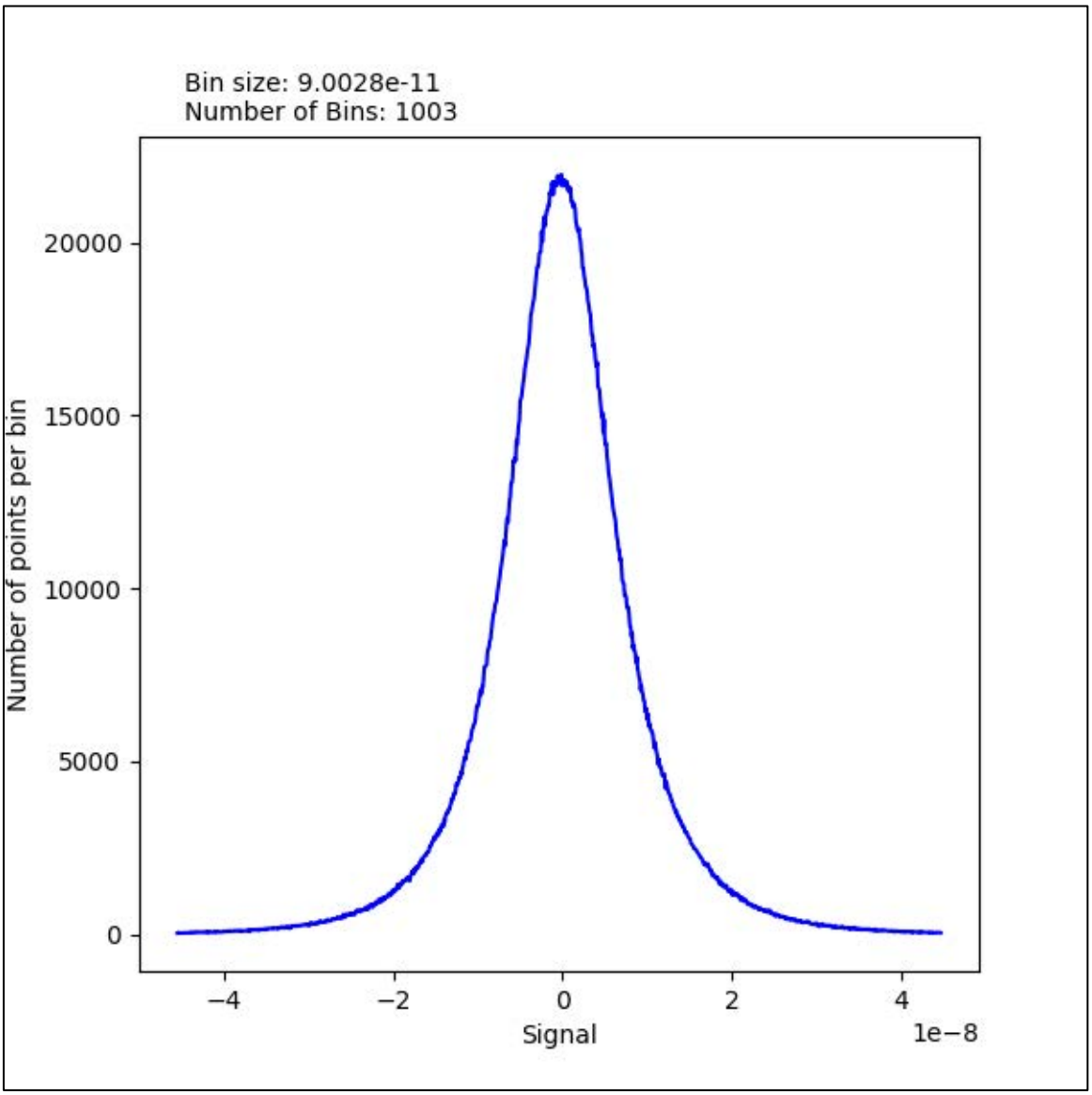

Figure 10: The histogram of median ramp curvature values from Figure 9.

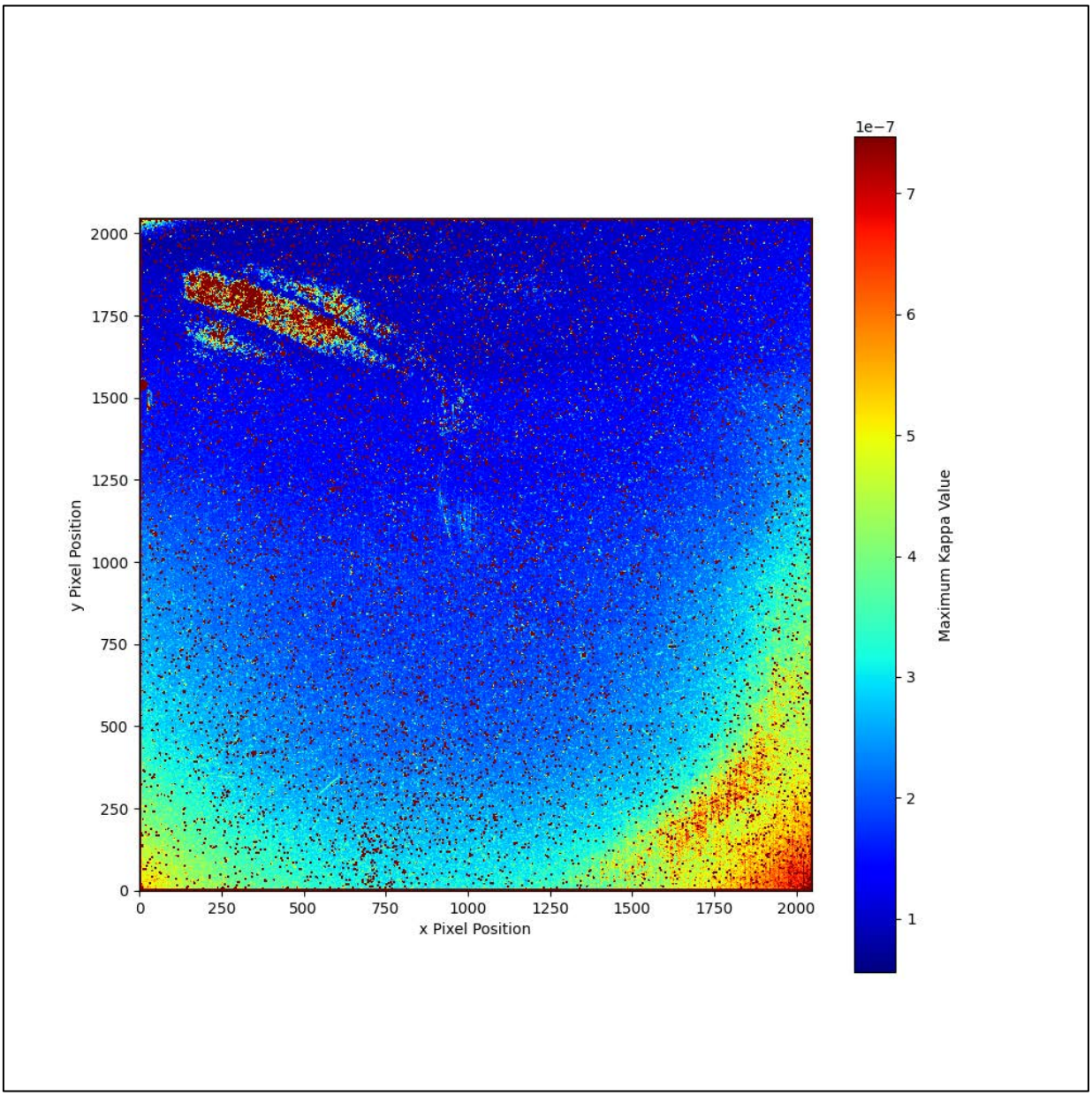

Figure 11: An image of the pixel-by-pixel maximum curvature values in ramp 1 of observation 3.

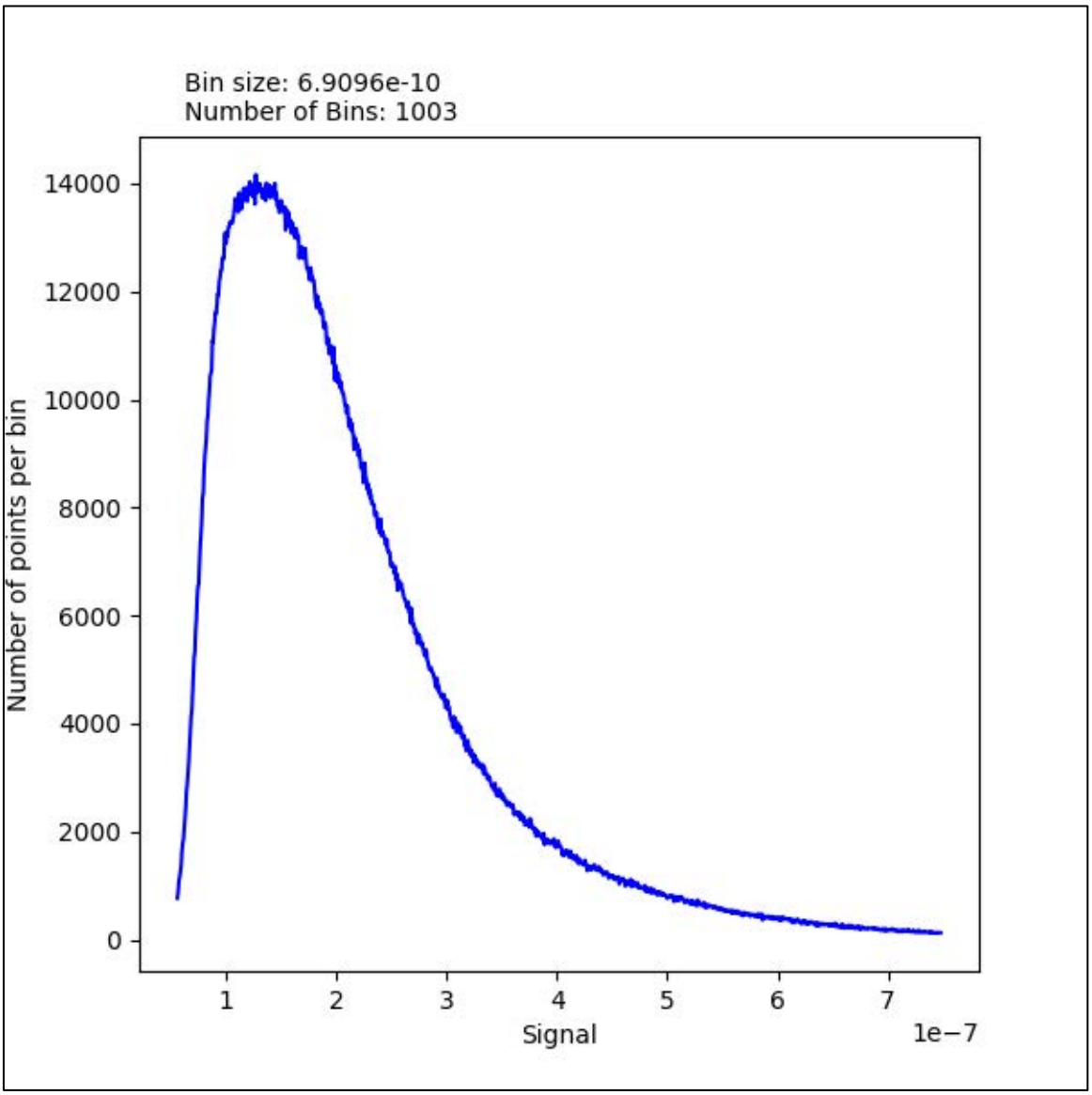

Figure 12: The histogram of the maximum curvature values from Figure 11.

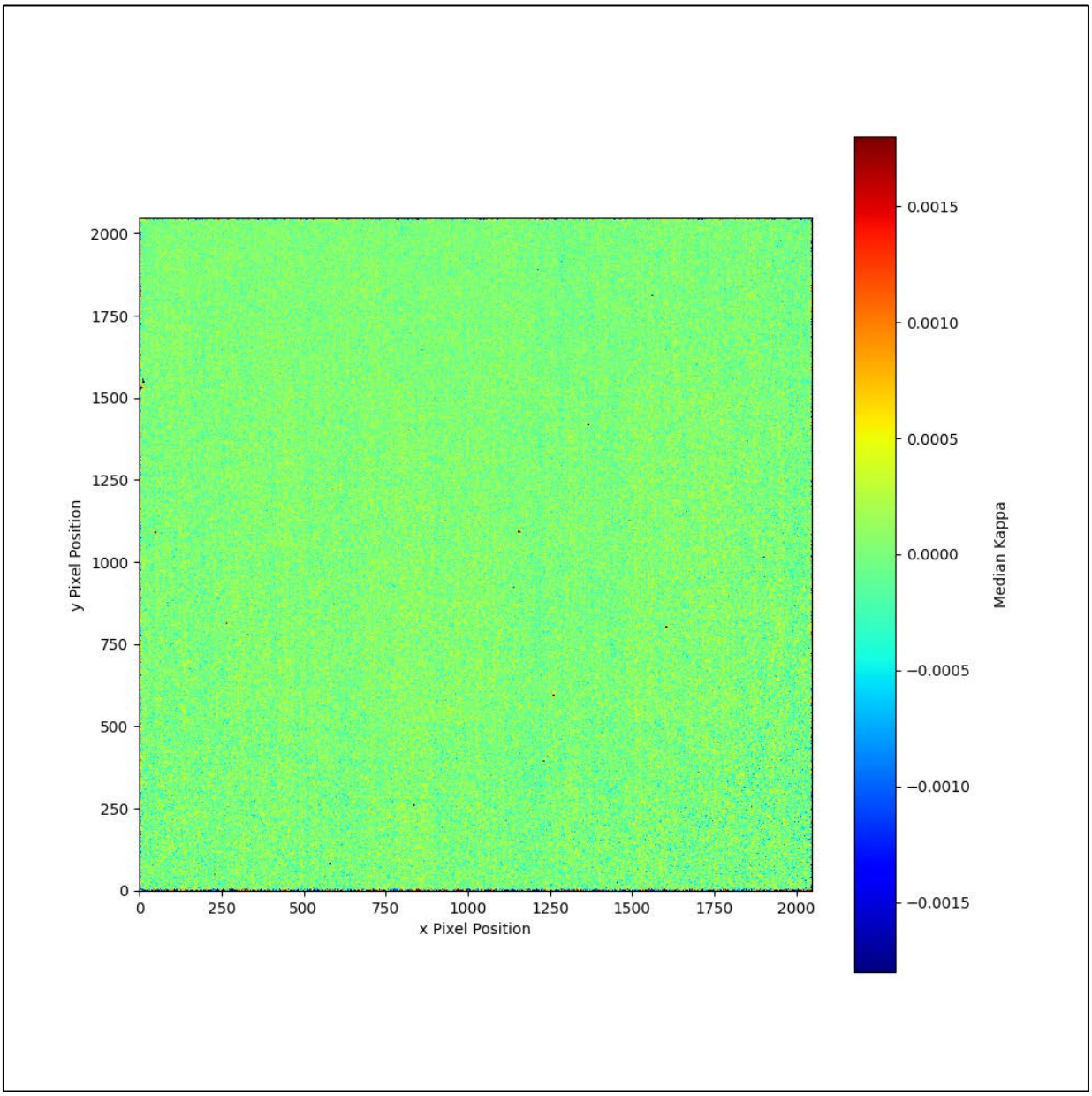

Figure 13: The median curvature values derived from the first difference frames in ramp 1 of observation 3. There is no evidence of large-scale structure across the array, but there are local pixel-to-pixel variations at any position.

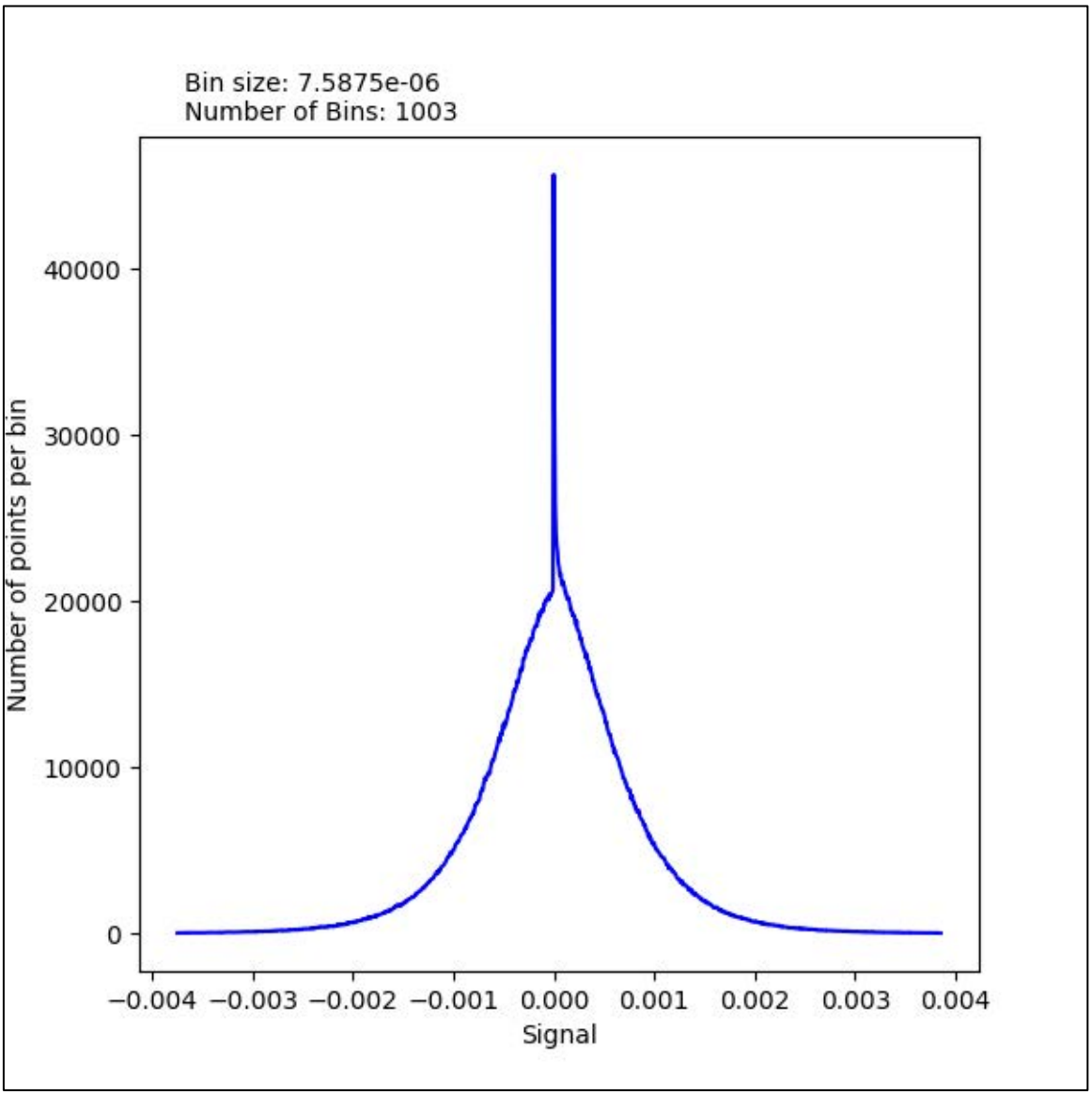

Figure 14: The histogram of the median first difference curvature values in Figure 13.

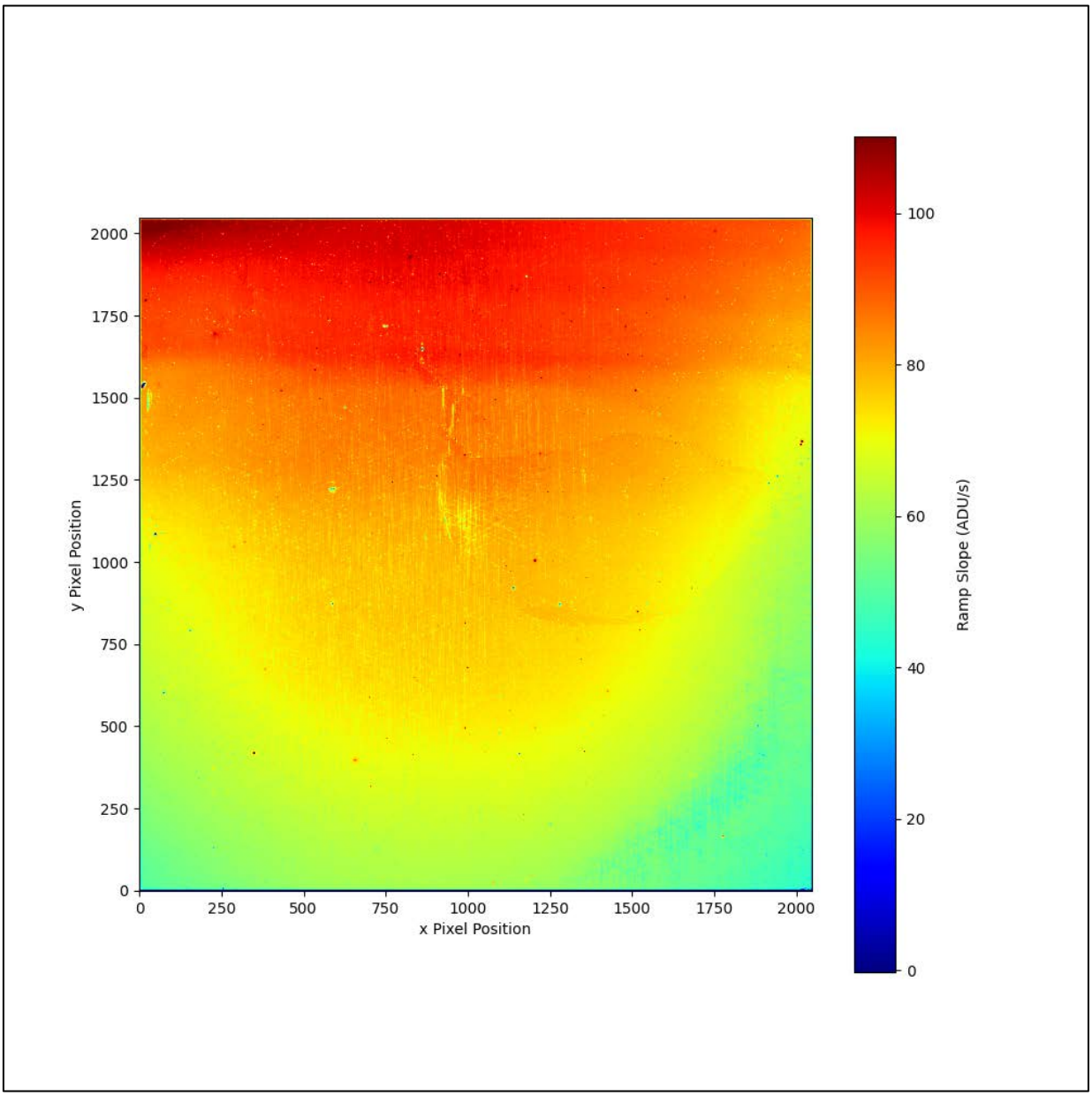

Figure 15: The ramp slope image from ramp 1 of observation 3.

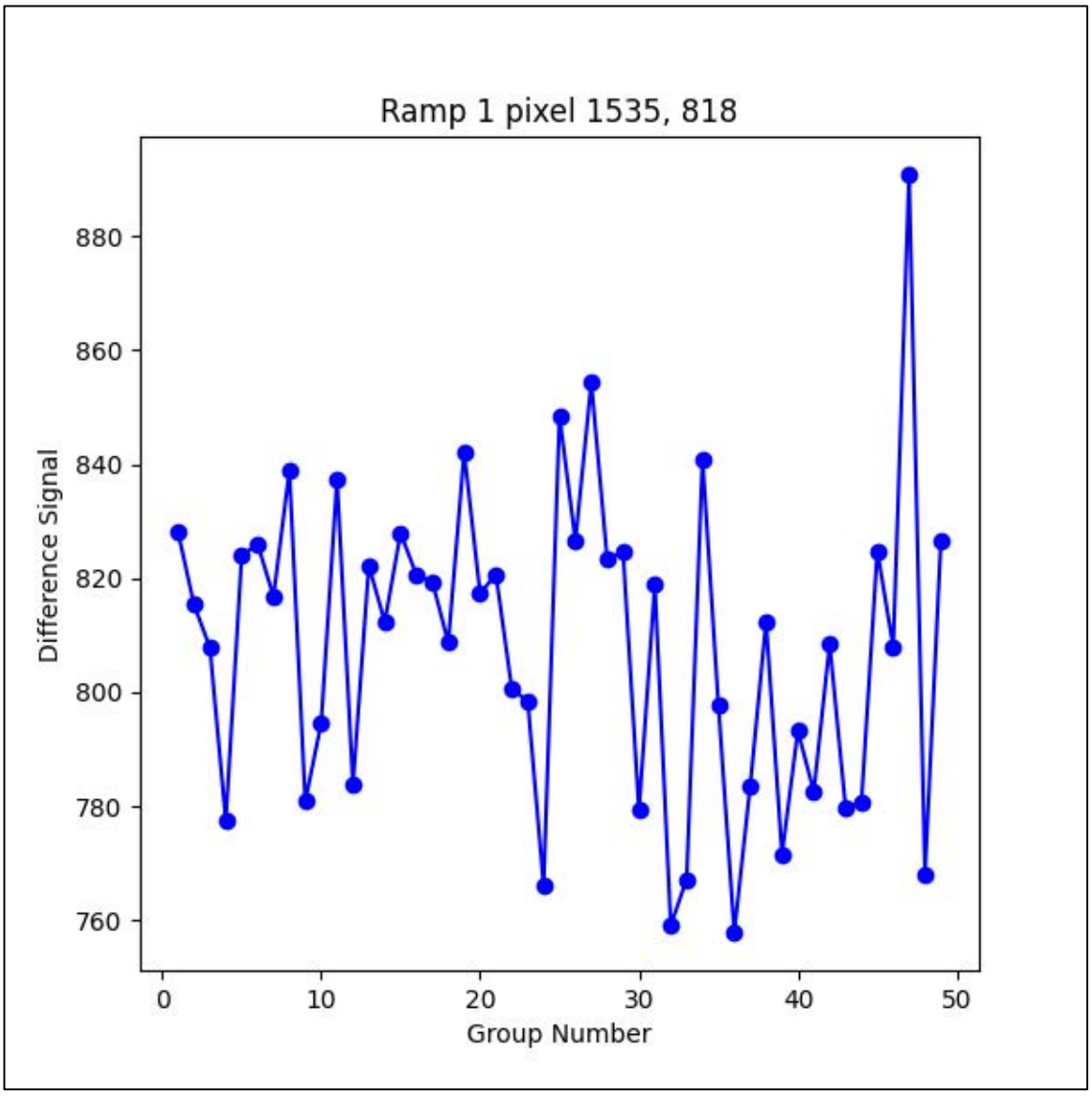

Figure 16: An example of the first difference frames in ramp 1 of observation 3, from a randomly selected pixel. The nominal standard deviation of the signal values is 22.5 ADU at this signal level.

6 Conclusions

The gain value over the NIRISS detector was calculated using 6 ramps from two internal flat lamp exposures taken as part of NIRISS commissioning program 1084 and found to be largely consistent with several gain maps made using ground-based testing data. The median gain from NIS-009 analysis for the entire illuminated area of the detector is 1.536 ± 0.064 e-/ADU. This median is within one standard deviation of the most comparable ground-based data: CV3 internal gain maps from 10-group ramps and 6-group ramps, respectively. The NIS-009 median gain is within 5% of all the ground-based gain calculations. Due to the higher precision of the CV3 external-lamp flat gain calculation, we will continue to use that value for NIRISS calibration.

Ramps were linearized using the current linearity reference file and for most of the pixels aside from ones flagged as bad in the pipeline the ramps were found to have small curvature values consistent with the random errors of the data points. This indicates that an update to the linearity reference file is not necessary based on these data.

7 References

Cooper, R.A., Wolfe, M.A., Volk, K. 2020, Description of the NIRISS Gain Reference File, JWST-STScI-005661

Martel, A.R. 2020, Analysis of the NIRISS Detector Void in the CV3 and OTIS Cryo Campaigns, JWST-STScI-007123

Volk, K. 2017, Analysis of NIRISS CV3 Data: Detector Gain Measurements, JWST-STScI-004823

8 Appendix

Data locations (as of September 2022):

1. CV3 internal flat gain maps (GitLab code):
    a. 3 ints, 10 groups
        i. IPC corrected, patched, smoothed: /ifs/jwst/wit/niriss/rcooper/nis_009_prep/internal_cv3_gain/OTP72_FLAT2_LEVEL5_NINTS3_NGROUPS10/niriss_ref_gain.fits
        ii. Non-smoothed: /ifs/jwst/wit/niriss/rcooper/nis_009_prep/internal_cv3_gain/OTP72_FLAT2_LEVEL5_NINTS3_NGROUPS10/internal_unsmooth/niriss_ref_gain.fits
    b. 3 ints, 35 groups (first 6 groups used)
        i. IPC corrected, patched, smoothed: /ifs/jwst/wit/niriss/rcooper/nis_009_prep/internal_cv3_gain/OTP72c_FLAT2_LEVEL6_NINTS3_NGROUPS35/niriss_ref_gain.fits
        ii. Non-smoothed: /ifs/jwst/wit/niriss/rcooper/nis_009_prep/internal_cv3_gain/OTP72c_FLAT2_LEVEL6_NINTS3_NGROUPS35/internal_unsmooth/niriss_ref_gain.fits
2. CV3 internal flat gain maps (Martel's code):
    a. 3 ints, 10 groups
        i. /ifs/jwst/wit/niriss/martel/gain/OTP72_FLAT2_LEVEL5_NINTS3_NGROUPS10/map_gain20_20.fits
    b. 3 ints, 35 groups (first 6 groups used)
        i. /ifs/jwst/wit/niriss/martel/gain/OTP72c_FLAT2_LEVEL6_NINTS3_NGROUPS35/map_gain20_20.fits